

Universal Rephasing Dynamics after a Quantum Quench via Sudden Coupling of Two Initially Independent Condensates

Emanuele G. Dalla Torre,¹ Eugene Demler,¹ and Anatoli Polkovnikov²

¹*Department of Physics, Harvard University, Cambridge MA 02138*

²*Department of Physics, Boston University, Boston MA 02215*

We consider a quantum quench in which two initially independent condensates are suddenly coupled, and study the subsequent “rephasing” dynamics. For weak couplings, the time-evolution of physical observables is predicted to follow universal scaling laws, connecting the short-time dynamics to the long-time non-perturbative regime. We first present a two-mode model valid in two and three dimensions and then move to one dimension, where the problem is described by a gapped Sine-Gordon theory. Combining analytical and numerical methods, we compute universal time-dependent expectation values, allowing a quantitative comparison with future experiments.

PACS numbers: 03.75.Kk, 05.70.Jk, 37.25.+k, 74.40.Gh

Equilibrium systems near second-order phase transitions are the best known examples of universal behavior in many-body physics. For these systems, universality implies that all macroscopic quantities are related to the distance from the transition point through universal critical exponents. In recent years, many efforts have been dedicated to the extension of these concepts to quantum systems out of thermal equilibrium (see for example Refs. [1–3] for open systems and Ref. [4] for a review on closed systems). In particular, some authors considered closed systems that are slowly driven through a second-order phase transition and, extending the Kibble-Zurek argument, found universal scaling laws of static and dynamic quantities [5–8]. Others considered sudden quenches and predicted a universal scaling of physical observables at long times after the quench [9–12]. Here we extend these arguments by demonstrating a universal behavior in the transient dynamics following a sudden quench, both at short and long times.

In this paper we consider systems that are initially prepared in the ground state of a gapless Hamiltonian, and that are quenched by the sudden opening of an excitation gap Δ (see Fig. 1(a)). In the Renormalization Group (RG) language, this corresponds to the sudden switching-on of a “relevant” perturbation. The resulting dynamics is described by a strongly interacting theory and is intrinsically non-perturbative [13]. Experimentally, this can be realized for example by preparing two independent Bose-Einstein condensates in their respective ground states and then suddenly switching-on a finite tunneling coupling j_{\perp} (see Fig. 1(b)). This opens an excitation gap for the relative-phase modes, given at a mean field level by the plasma frequency $\Delta = 2\sqrt{\mu j_{\perp}}$, where μ is the chemical potential. Beyond-mean-field effects will be extensively discussed below.

In the limit of $j_{\perp} \ll \mu$, the dynamics following the quench is dominated by the low-frequency modes and is thus expected to be universal. For a generic physical observable $C(t)$ we predict the universal contributions to have the form

$$C(t) = \left(\frac{\Delta}{\mu}\right)^{\eta} R(\Delta t) . \quad (1)$$

Here η is the scaling dimension corresponding to the spe-

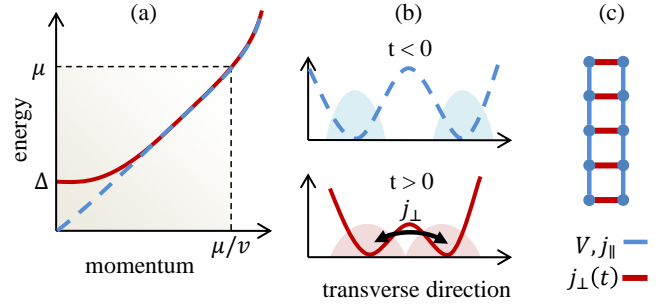


FIG. 1: [Color online] (a) Dispersion relation before (dashed) and after (solid) a quantum quench opening a gap Δ and involving only the low-frequency modes. (b) Physical realization: sudden coupling of two independent condensates via a uniform tunneling j_{\perp} . (c) Lattice model used for the numerical calculations.

cific observable and R is a scaling function, fixing the universal behavior of the transient many-body dynamics. As we will demonstrate, the scaling ansatz (1) is valid at times both shorter and longer than the inverse gap $1/\Delta$. This allows to extract information about the non-perturbative long-time dynamics from the short-time dynamics, where time-dependent perturbation theory applies. A similar relation is known to hold for classical systems, with important theoretical and computational applications [14–17].

Two and three dimensions – To substantiate our predictions we first apply a two-mode model, valid in two and three dimensions [49]. Further conditions for the validity of this model are discussed towards the end of the paper. By considering only the macroscopically occupied state of each condensate, we describe the sudden quench by:

$$H(t) = \frac{\mu}{N} (\delta n_1^2 + \delta n_2^2) - \Theta(t) j_{\perp} (\psi_1^{\dagger} \psi_2 + \text{H.c.}) . \quad (2)$$

Here $\delta n_{\alpha} = \psi_{\alpha}^{\dagger} \psi_{\alpha} - N_{\alpha}$, with $N_{\alpha} = N/2$; ψ_{α} , with $\alpha = 1, 2$, is a canonical bosonic operators, and $\Theta(t)$ is the Heaviside step function. The two terms in Eq. (2) describe respectively the interactions among the atoms in the same condensate and the sudden switching-on of a tunneling coupling. Results from the exact diagonalization of Eq. (2) for different values of j_{\perp}

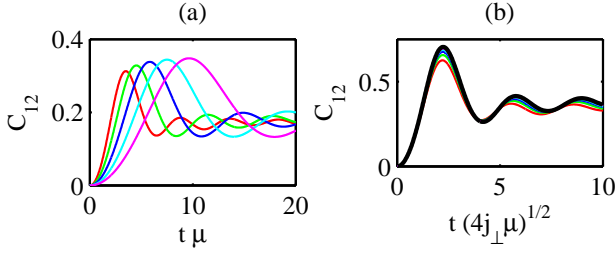


FIG. 2: [Color online] Time evolution of the interference contrast $C_{12}(t) = \langle \psi_1^\dagger \psi_2 + \text{H.c.} \rangle / 2N = \langle \cos(\sqrt{2}\phi) \rangle$, according to the two-mode quantum Hamiltonian (2) with $N = 1000$. (a) Exact diagonalization for different values of the ratio $j_{\perp}/\mu = 0.10$ (red), 0.060 (green), 0.037 (blue), 0.022 (cyan), 0.0135 (magenta). (b) Same plots on rescaled axes, showing the universal behavior (1) with $\eta = 0$, superimposed to the analytic solution of the simple pendulum (thick solid line).

are shown in Fig. 2(a). Subplot (b) shows the data collapse obtained by rescaling the time axis, and demonstrating the validity of our scaling ansatz (1), with $\eta = 0$.

To understand the observed scaling behavior, it is useful to introduce the phase fields ϕ_α , canonically conjugate to δn_α , through the approximate relation $\psi_\alpha \approx \sqrt{N_\alpha} e^{i\phi_\alpha}$. Moving to the relative coordinates $\phi = (\phi_1 - \phi_2)/\sqrt{2}$ and $n = (\delta n_1 - \delta n_2)/\sqrt{2}$, we obtain the Josephson junction Hamiltonian

$$H(t) = \frac{2\mu}{N} n^2 - 2\Theta(t) j_{\perp} N \cos(\sqrt{2}\phi). \quad (3)$$

The ground state and first-few excited states of the final Hamiltonian $H(t > 0)$ are well described by the harmonic approximation $\cos(\sqrt{2}\phi) \approx 1 - \phi^2$. When applied to the present quench, this approximation predicts undamped oscillations with frequency $\Delta = 2\sqrt{\mu j_{\perp}}$. Instead, as shown in Fig. 2, the universal dynamics displays strongly damped oscillations. The harmonic approximation breaks down because the initial state $|n=0\rangle$ has a large overlap with a macroscopic number of eigenstates of the final Hamiltonian, $N_{\text{excited}} = N \sqrt{j_{\perp}/\mu} \gg 1$. For these states all higher-order Taylor components of the cosine need to be considered, highlighting the strongly interacting nature of the predicted dynamics.

In the limit of large N , an alternative, non-perturbative description is available: the semiclassical approach, or Truncated Wigner approximation [18–20]. Following this method (see Appendix), we map the quantum Hamiltonian (3) to the classical equations of motion of a simple pendulum $d^2\phi/dt^2 = -\Delta^2 \sin(\sqrt{2}\phi)/\sqrt{2}$, whose analytical solution is known. The quantum nature of the problem enters through the initial conditions, for which ϕ is uniformly distributed between zero and $\sqrt{2}\pi$. The resulting dynamics corresponds to damped oscillations with a single frequency scale Δ and correctly reproduces the numerical solution of the full quantum model, as shown in Fig. 2(b).

One dimension – In one dimension the initial state is not described by two macroscopically occupied modes, but rather by two “quasi-condensates” with power-law correlations. Using the standard bosonization technique [21], we describe the system in terms of two phase *fields*, $\phi_1(x, t)$ and $\phi_2(x, t)$, and

the time-dependent Hamiltonian

$$H = \sum_{\alpha=1,2} H_{LL}[\phi_\alpha] - 2j_{\perp}(t) \rho_0 \int dx \cos(\phi_1 - \phi_2). \quad (4)$$

Here the first term describes the low-frequency modes of the two independent condensates as “Tomonaga-Luttinger liquids” [22] with sound velocity v and Luttinger parameter K . The latter measures the ratio between the longitudinal kinetic energy and the interaction energy: $K \rightarrow \infty$ corresponds to free bosons and $K = 1$ to the Tonks-Girardeau limit. The second term of Eq. (4) describes the tunneling between the two condensates, according to the “bosonization dictionary” $\psi_\alpha \rightarrow \sqrt{\rho_0} e^{i\phi_\alpha}$.

Introducing the relative coordinate $\phi = (\phi_1 - \phi_2)/\sqrt{2}$ we obtain the well-known “Sine-Gordon” model with a nonlinear term proportional to the cosine of the relative phase, $\cos(\phi_1 - \phi_2) = \cos(\sqrt{2}\phi)$. At zero temperature, this model is characterized by a quantum phase transition between the gapless Tomonaga-Luttinger liquid ($K < 1/4$) and a gapped phase ($K > 1/4$). The effects of the quench in the two phases are very different. For $K < 1/4$, the cosine is irrelevant in an RG sense and the low-frequency dynamics is governed by the quadratic Luttinger liquid theory (i.e. the first term of the Hamiltonian (4)). At long times, this theory predicts the appearance of universal power-laws [12, 23]. In contrast, for $K > 1/4$, the cosine is relevant and the resulting theory is strongly interacting [50]. As we will now show, in this case the dynamics is universal both at short and long times.

To study the dynamics of the problem we first perform a series expansion in the tunneling coupling j_{\perp} . Moving to a path-integral formulation of the problem (for an introduction see for example Refs. [24, 25]), we represent the Hamiltonian (4) in terms of the real-time action:

$$S = \int_{\gamma_K} dt \int dx \frac{K}{\pi} [(\partial_x \phi)^2 - (\partial_t \phi)^2] + 2\Theta(t) j_{\perp} \rho_0 \cos(\sqrt{2}\phi). \quad (5)$$

Here γ_K is the Keldysh contour and we switched to units where $v = 1$. Splitting the Keldysh contour in its forward and backward branches (ϕ_+ and ϕ_- respectively) and moving to their symmetric and anti-symmetric combinations (defined by $\phi_{\pm} = \phi \pm \hat{\phi}$ and often termed “classical” and “quantum” components), we have:

$$\begin{aligned} 2 \int_{\gamma_K} dt \cos(\sqrt{2}\phi) &= 2 \int dt \cos(\sqrt{2}\phi_+) - \cos(\sqrt{2}\phi_-) \quad (6) \\ &= 4 \int dt \sin(\sqrt{2}\phi) \sin(\sqrt{2}\hat{\phi}) = \sum_{\epsilon=\pm, \hat{\epsilon}=\pm} \int dt e^{\sqrt{2}\epsilon\phi + \sqrt{2}\hat{\epsilon}\hat{\phi}}. \end{aligned}$$

Expanding e^{iS} in a Taylor series around $j_{\perp} = 0$ we obtain

$$\begin{aligned} C_{12}(t) &\equiv \langle \cos(\sqrt{2}\phi(t)) \rangle \\ &= \text{Re} \langle e^{\sqrt{2}i\phi} \sum_N \frac{(i j_{\perp} \rho_0)^N}{N!} \left(\sum_{\epsilon, \hat{\epsilon}} \int_0^\infty dt \int_{-\infty}^\infty dx e^{\sqrt{2}i(\epsilon\phi + \hat{\epsilon}\hat{\phi})} \right)^N \rangle. \quad (7) \end{aligned}$$

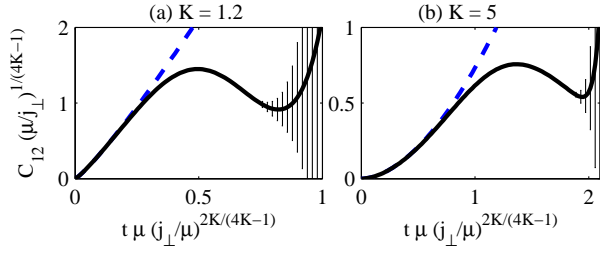


FIG. 3: [Color online] Series expansion (9). Numerical results obtained by keeping the first N_{\max} terms of the series (solid curve and error-bars) and analytic results (see Appendix) for the first-order contribution $N = 1$ (dashed curve). (a) $K = 1.2$, $N_{\max} = 11$; (b) $K = 5$, $N_{\max} = 23$. In both cases we used 10^6 random evaluation points of $\{(x_i, t_i)\}_{i=1}^N$.

Note that the N -th term of Eq. (7) contains $2N$ continuous integrals and $2N$ discrete sums, whose dummy indexes we will denote as $(x_i, t_i, \epsilon_i, \hat{\epsilon}_i)$ with $i = 1, \dots, N$. In analogy to the equilibrium case [26, 27], we can interpret the first three elements as the space-time coordinates and charges of a Coulomb gas with N particles (dual to the atoms of the original problem). In contrast, the $\hat{\epsilon}_i$ indexes do not have an equilibrium analogue and rather impose a light-cone constraint (see Appendix), limiting all contributing “charges” to the past-light-cone of (x, t) , or $|x - x_i| < t - t_i$. This light-cone effect is generic to global quantum quenches (see for example Refs. [23, 28]) and prevents the exact mapping to an equilibrium model.

The expectation value appearing in Eq. (7) refers to the initial state, corresponding to the ground state of two independent Luttinger liquids, and can be computed using the quadratic part of Eq. (5). After rescaling the time and space variables of integration (see Appendix), we arrive to

$$C_{12}(t) = \sum_N c_N \left(\frac{j_{\perp}}{\mu}\right)^N (\mu t)^{2N-(N+1)/(2K)} \quad (8)$$

$$= \left(\frac{j_{\perp}}{\mu}\right)^{1/(4K-1)} \sum_N c_N \left[(j_{\perp}/\mu)^{2K/(4K-1)} \mu t\right]^{2N-(N+1)/(2K)}. \quad (9)$$

The coefficients c_N are universal: they do not depend neither on the cutoff nor on j_{\perp} .

To achieve a universal scaling of the form of Eq. (1) it is necessary to rescale the time in units of the inverse gap. For the Sine-Gordon model, the excitation gap can be exactly computed using the form-factor approach [29] and, in our notations, it is proportional to $\Delta = \mu(j_{\perp}/\mu)^{2K/(4K-1)}$, leading to

$$C_{12}(t) = \left(\frac{\Delta}{\mu}\right)^{\eta} \sum_N c_N (\Delta t)^{2N-(N+1)/(2K)} \equiv \left(\frac{\Delta}{\mu}\right)^{\eta} R(\Delta t). \quad (10)$$

with $\eta = 1/(2K)$. Remarkably, we obtain the same “anomalous” scaling dimension η as in the ground state of the model [30]. This result corroborates with a scaling analysis [31] showing that the average amount of energy-per-mode introduced by the quench scales to zero much faster than the gap.

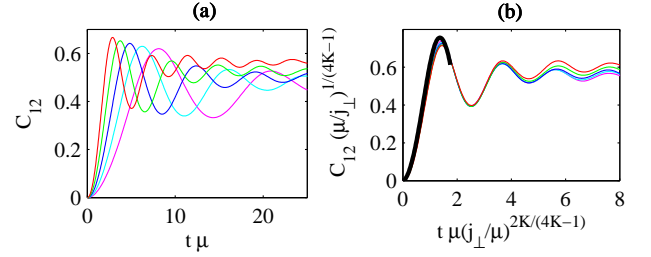


FIG. 4: [Color online] Truncated Wigner approach (11). (a) Numerical results for $j_{\perp}/\mu = 0.27$ (red), 0.16 (green), 0.10 (blue), 0.060 (cyan), 0.036 (magenta) with $K = 5$, system size $L = 400$, number of random paths $M = 400$. (b) Data-collapse according to Eq. (10), superimposed to the result from the series expansion (black curve, identical to Fig. 3(b)).

In the above derivation we used the asymptotic values of correlation and response functions, related to the low-frequency modes, and we neglected the contributions from the high-frequency modes. These non-universal contributions are analytic functions of the bare parameters. As such, they can at most contribute to C_{12} a term that is linearly proportional to j_{\perp} . In contrast, the universal contributions scale at long times as $j_{\perp}^{1/(4K-1)}$ and are therefore dominant for any $K > 1/2$. Remarkably, the intermediate case of $K = 1/2$ can be exactly solved by mapping the problem to non-interacting fermions [32]. Indeed, at this point, the universal and non-universal contributions scale in the same way and the latter are no more negligible.

At present, we were not able to compute the universal function R by the analytic resummation of the series (9). Instead, we numerically estimate its first few terms by averaging over random samplings of (ϵ_i, x_i, t_i) . The resulting universal curves are shown in Fig. 3 for two different values of K . Our calculations are presently limited to time scales of order $1/\Delta$ due to a “dynamical sign problem”, related to the alternating signs of the coefficients c_N . To predict the universal behavior at longer times, we will now present two alternative numerical methods.

The first method extends the semiclassical approach presented above for the two-mode model. The corresponding classical equation of motion is [13]

$$\partial_t^2 \phi = \partial_x^2 \phi - \frac{2\pi}{K} j_{\perp} \rho_0 \sin(\sqrt{2} \phi). \quad (11)$$

The numerical solution of this equation is in good agreement with the series expansion and extends to longer times, as shown in Fig. 4 for $K = 5$. Note however that Eq. (11) is characterized by a single energy scale $\sqrt{2\pi j_{\perp} \rho_0 / K} \sim j_{\perp}^{1/2}$, matching the excitation gap of the original quantum model only for $K \gg 1$. As expected, the semiclassical approach breaks down for $K \sim 1$, where the correspondent equilibrium system approaches a quantum phase transition.

To describe the regime $K \sim 1$, we map the problem into a lattice model and apply one of the derivatives of the Density Matrix Renormalization Group (DMRG) algorithm [33, 34]. This approach is well suited to situations, as the one un-

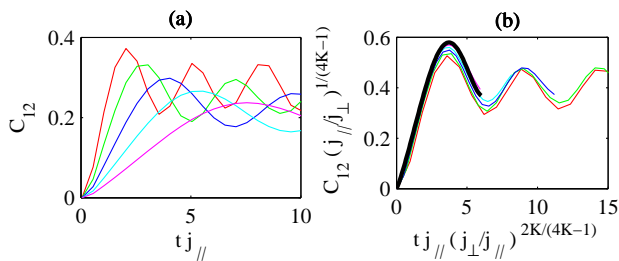


FIG. 5: [Color online] Hard-core bosons model (12). (a) Numerical results for $j_{\perp}/j_{\parallel} = 0.27$ (red), 0.16 (green), 0.10 (blue), 0.060 (red), 0.036 (cyan), 0.022 (magenta), with $V/j_{\parallel} = -1/2$, or $K = \pi/(2\pi - 2 \arccos(V/2j_{\parallel})) \approx 1.2$. The calculations were performed using the Time Evolving Block Decimation (TEBD) algorithm of Refs. [37, 38] for system size $L = 100$, number of states $\chi = 100$ and took around three days/curve on a single core. (b) Data collapse according to Eq. (10), superimposed to the result from the series expansion (black curve, identical to Fig. 3(a) after the appropriate rescaling).

der present consideration, in which the time evolution is performed with a *gapped* Hamiltonian. To minimize the memory requirements we consider hard-core bosons on a ladder (see Fig. 1(c)) represented by the Hamiltonian

$$H(t) = \sum_{L=1}^N \left[\sum_{\alpha=1,2} -j_{\parallel} (b_{\alpha,i}^{\dagger} b_{\alpha,i+1} + \text{H.c.}) + V n_{\alpha,i} n_{\alpha,i+1} \right] - \Theta(t) j_{\perp} (b_{1,i}^{\dagger} b_{2,i} + \text{H.c.}) . \quad (12)$$

Here the energy scale j_{\parallel} sets the chemical potential and $V < 0$ is a nearest neighbor *attractive* interaction, meant to partially counter-balance the hard-core constraint [51]. For $j_{\perp} = 0$ the two independent chains are Bethe-ansatz [35] solvable, allowing to exactly determine the Luttinger parameter [22, 36]. The numerical simulation of the model (12) is presented in Fig. 5 and confirms our scaling ansatz (see the caption for details).

Discussion and conclusion – In contrast to the above-mentioned models, actual experiments necessarily involve a finite initial temperature T_0 and a finite quench time τ . Intuitively, one may expect the idealized model of a sudden quench to hold only as long as τ is smaller than the inverse of the energy of the highest excited state. For the Hamiltonian (3) this energy scale is $N_{\text{excited}} \Delta \sim N j_{\perp}$, leading to the requirement $\tau \ll 1/(N j_{\perp})$. However, as discussed in Ref. [39], the most probable excitation path does not directly connect the ground state to the highest excited state, but is rather given by subsequent steps connecting neighboring levels, each with energy splitting Δ . This observation indicates that the more lenient condition $\tau \ll 1/\Delta$ is sufficient to observe a universal behavior. A similar scaling argument holds for the initial temperature T_0 , which needs to be smaller than Δ . These two constraints, $\tau \ll 1/\Delta$ and $T \ll \Delta$, should be combined with the weak coupling condition $\sqrt{j_{\perp}/\mu} = \Delta/\mu \ll 1$, requiring temperatures (ramp times) smaller than the (inverse) chemical potential by one order of magnitude. These conditions are in the reach of present experiments with ultracold neutral atoms (see also the Appendix for the details of a possible realization

with wave-interferometers of atoms on a chip [40, 41]).

A final and important question regards the coupling to the modes that have been neglected in the model Hamiltonians (2) and (4). In particular, the former does not include Bogoliubov excitations and the latter neglects the coupling to the “symmetric” mode $\bar{\phi} = (\phi_1 + \phi_2)/\sqrt{2}$. These low-frequency modes may act as a dissipative bath for the relative-phase ϕ and lead to a further “rephasing”. A complete analysis of their effect goes beyond the scope of the present Letter. At this stage we can only comment that, based on the analogy with the equilibrium case, one should expect the couplings to these additional modes to be irrelevant in an RG sense and thus to effect the dynamics only at time scales much larger than Δ . Accordingly, the life-time of the predicted “prethermalized” state should tend to infinity as one approaches the weak-coupling limit $j_{\perp}/\mu \rightarrow 0$.

In summary, we studied the many-body quantum dynamics of two initially independent condensates, suddenly coupled via uniform tunneling (“global quench”). In two and three dimensions we applied a “two-mode” model, while in one dimension we mapped the problem to a gapped Sine-Gordon model. Both theories are strongly interacting and lead to non-perturbative dynamics. We determined the scaling laws for expectation values of physical observables and predicted a universal time-dependence, connecting short and long times. Our findings may have important implications for both numerical calculations and experiments, in which the long-time evolution is hard to achieve. They may also allow to perform finite-size scaling and renormalization-group analysis in the time domain [42–45], in analogy to the established equilibrium techniques.

We wish to thank J. Simon for many useful insights on the experimental realization and C. De Grandi, D. Huse, C. Karrasch, D. Schuricht, Shuyuan Wu for critically reading the manuscript. We also acknowledge useful discussions with E. Altman, E. Berg, I. Bloch, T. Giamarchi, P. Le Doussal, D. Orgad, C. Neuenhahn. We acknowledge support from Harvard-MIT CUA, NSF Grants No. DMR-07-05472 and DMR-09-07039, DARPA OLE program, AFOSR Quantum Simulation MURI and AFSOR FA9550-10-1-0110, the ARO-MURI on Atomtronics, Sloan Foundation, Simons Foundation. Finally, we would like to thank the KITP for hospitality during the workshop on “Quantum Dynamics in Far from Equilibrium Thermally Isolated Systems”.

Appendix A: Derivation of the semiclassical equations of motion from Eq. (3)

Consider the generic quantum time-dependent Hamiltonian

$$H(t) = \frac{\mu}{2N} p^2 + 2N j_{\perp} f(t) V(x), \quad (A1)$$

where x , p are unitless canonical variables, and $V(x)$, $f(t)$ are unitless functions. For the ramp of a Josephson junction ,

$V(x) = \cos(x)$ and

$$f(t) = \begin{cases} t/\tau & t < \tau \\ 1 & t > \tau \end{cases} \quad (\text{A2})$$

The correspondent action is:

$$S[x, p] = S_0 + i \int_{\gamma_K} dt p \partial_t x - \frac{\mu}{2N} p^2 - 2N j_{\perp} f(t) V(x), \quad (\text{A3})$$

where γ_K runs over the contour ($0 \rightarrow +\infty \rightarrow 0$) and $e^{iS_0} = \langle \psi_0 | p_0^+, x_0^+ \rangle \langle p_0^+, x_0^+ | \psi_0 \rangle$ sets the initial conditions. If the initial state is $|p=0\rangle$, we have

$$e^{iS_0} = \delta(p_0^+) \delta(p_0^-) \delta(x^+ - x^-) \quad (\text{A4})$$

After integrating-out the p variable we get:

$$S[x, p] = S_0 + iN \int_{\gamma_K} dt \frac{1}{2\mu} (\partial_t x)^2 - 2j_{\perp} f(t) V(x) \quad (\text{A5})$$

In the limit of $N \rightarrow \infty$, only the saddle point contributes to the path integral. Here, the saddle point corresponds to the classical equation of motions

$$\partial_t^2 x = 2\omega_0 f(t) V'(x) \quad (\text{A6})$$

with initial conditions substituted by the distribution function $P(x_0, t_0) = e^{iS_0[x_0, \partial_t x_0]}$. Note that the microscopic energy scales $J = j_{\perp} N$ and $U = \mu/N$ completely disappeared from the problem.

Appendix B: Technical details of the ‘‘Coulomb gas’’ expansion Eq. (8)

The starting point of the present derivation is Eq. (7). If we define $\phi_0 = \phi(x, t)$, $\epsilon_0 = \hat{\epsilon}_0 = 1$ and use the compact notation $\sum_N = \sum_{N, \{\epsilon_i, \hat{\epsilon}_i\}}$, and $\int_N = \prod_{i=1}^N \int_0^{\infty} dt_i \int_{-\infty}^{\infty} dx_i$, we can express the interference contrast as

$$C_{12}(t) = \sum_N \frac{(j_{\perp} \rho_0)^N}{N!} \int_N \epsilon_i \hat{\epsilon}_i \langle \exp \left(\sqrt{2}i \sum_{i=0}^N \epsilon_i \phi_i + \hat{\epsilon}_i \hat{\phi}_i \right) \rangle \quad (\text{B1})$$

The expectation value refers to the initial state, given by the ground state of two independent Luttinger liquids, and can be computed from the action (5) with $j_{\perp} = 0$. Dealing with a quadratic action, we can apply Wick’s theorem

$\langle e^{iA} \rangle = \langle e^{-\langle A^2 \rangle / 2} \rangle$ and obtain

$$C_{12}(t) = \sum_N \frac{(j_{\perp} \rho_0)^N}{N!} \int_N \epsilon_i \hat{\epsilon}_i \exp \left(- \left\langle \left(\sum_{i=0}^N \epsilon_i \phi_i + \hat{\epsilon}_i \hat{\phi}_i \right)^2 \right\rangle \right) \quad (\text{B2})$$

$$= \sum_N \frac{(j_{\perp} \rho_0)^N}{N!} \int_N \epsilon_i \exp \left(- \sum_{i,j=0}^N \epsilon_i \epsilon_j \langle \phi_i \phi_j \rangle \right) \times \hat{\epsilon}_i \exp \left(- \sum_{i,j=0}^N \epsilon_i \hat{\epsilon}_j \langle \phi_i \hat{\phi}_j \rangle \right), \quad (\text{B3})$$

where we used the identity $\langle \hat{\phi} \hat{\phi} \rangle = 0$, related to the causality constraint [25].

In one dimension, the correlation functions $\langle \phi_i \phi_j \rangle$ are infra-red divergent. As a consequence the above expression vanishes, unless $\sum_{i=0}^N \epsilon_i = 0$. If we interpret ϵ_i as the charges of a Coulomb gas, this condition coincides with the requirement of a total charge neutrality. It constraints $N+1$ to be even and $\prod_i \epsilon_i = (-1)^{(N+1)/2}$. This alternating sign will be the origin of a ‘‘sign problem’’, preventing the numerical resummation of the series.

We now assume that the largest contribution to integrals over time and space comes from the universal asymptotic behavior of the correlation functions [46]

$$\begin{aligned} \langle (\phi_i - \phi_j)^2 \rangle &= \frac{1}{8K} \log \left(\mu \left| (x_i - x_j)^2 - (t_i - t_j)^2 \right| \right) \\ \langle \phi_i \hat{\phi}_j \rangle &= \frac{\pi}{4K} \Theta(t_i - t_j - |x_i - x_j|) \end{aligned} \quad (\text{B4})$$

We discussed the non-universal short-distance behavior at the end of the paper and show that they indeed are negligible for $K > 1/2$.

Using Eq. (B4), we obtain that the second line of Eq. (B3) becomes

$$\hat{\epsilon}_j \exp \left(- \hat{\epsilon}_j \sum_{i=0}^N \epsilon_i \langle \phi_i \hat{\phi}_j \rangle \right) = -2i \sin \left(n_j \frac{\pi}{4K} \right). \quad (\text{B5})$$

Here we explicitly performed the sum over $\hat{\epsilon}_j$ and we defined n_j as the total charge of the points inside the future light cone of (x_j, t_j) . Note that $C_{12}(t)$ vanishes unless $n_j \neq 0$ for all $j = 1, \dots, N$. This condition can be fulfilled only if all the ‘‘charges’’ are inside the past light-cone of (x, t) , satisfying $|x - x_j| < t - t_j$. This ‘‘light-cone physics’’ is relevant to any global quantum quench (see f.e. Refs. [23, 28]) and highlights the difference between similar equilibrium Coulomb gas expansions.

The first line of Eq. (B3) equals to

$$\exp \left(-2 \sum_{i,j=0}^N \epsilon_i \epsilon_j \langle \phi_i \phi_j \rangle \right) = \prod_{i,j=0, i \neq j}^N \left| (x_i - x_j)^2 - (t_i - t_j)^2 \right|^{\epsilon_i \epsilon_j / (4K)}, \quad (\text{B6})$$

Note that there are $(N+1)N$ homo-sign combinations and $(N+1)(N+1)$ hetero-sign combinations, thus at long times this term is proportional to $(t^{1/2K})^{(N+1)N/2 - (N+1)(N+1)/2} =$

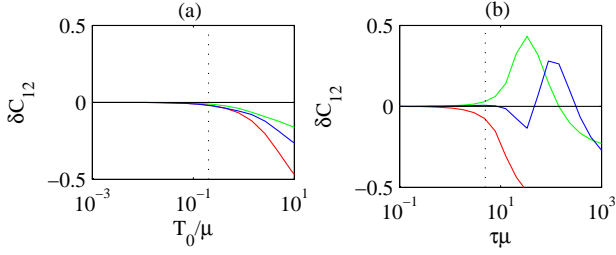


FIG. 6: [Color online] Comparison between the idealized case considered in Fig. 2 and (a) finite initial temperature T_0 , or (b) finite ramp time τ . The solid lines represent $\delta C_{12}(t) \equiv C_{12}^{\text{finite}}(t) - C_{12}^{\text{ideal}}(t)$ at different times $t = 10/\mu$ (red), $20/\mu$ (green), and $30/\mu$ (blue). The vertical dashed lines correspond to (a) $T_0 = \Delta$, (b) $\tau = 1/\Delta$. As predicted, the dynamics on the left side of these lines is independent of T_0 and τ . Numerical parameters – $j_{\perp}/\mu = 0.01$, $\Delta = 2\sqrt{j_{\perp}/\mu} = 0.2\mu$, and $N = 1000$.

$t^{-(N+1)/(2K)}$. To obtain Eq. (8) it is sufficient to rescale the time and space integration parameters $dt \rightarrow t dt$ and $dx \rightarrow t dx$.

The coefficients c_N are universal (do not depend neither on the cutoff nor on the gap) and are given by

$$c_N = \sum_{\{\epsilon_i = \pm\}} \frac{2^N (-1)^{\frac{N+1}{2}}}{N!} \prod_{i=1}^N \int_{-\infty}^{\infty} dx_i \int_0^{\infty} dt_i \sin\left(-n_i \frac{\pi}{2K}\right) \prod_{j \neq i}^N |(x_i - x_j)^2 - (t_i - t_j)^2|^{\epsilon_i \epsilon_j / (4K)}. \quad (\text{B7})$$

with $(x_0, t_0) = (0, 1)$ and $\epsilon_0 = 1$. The coefficient c_1 corresponds to the first order time-dependent perturbation theory and can be computed analytically

$$c_1 = 2 \sin\left(\frac{\pi}{2K}\right) \int_0^{\infty} dt \int_{-t}^t dx \frac{1}{|x^2 - t^2|^{1/(2K)}} \quad (\text{B8})$$

$$= \frac{2 \sin\left(\frac{\pi}{2K}\right) \sqrt{\pi} \Gamma\left(1 - \frac{1}{2K}\right)}{\left(2 - \frac{1}{K}\right) \Gamma\left(\frac{3}{2} - \frac{1}{2K}\right)}, \quad (\text{B9})$$

Here the second line has been computed with Wolfram's Mathematica (v8.0.1) and Γ is the Gamma function.

Appendix C: Finite temperature and finite ramp time

We now consider the effects of a finite initial temperature T_0 and a finite ramping time τ . Because the dynamics described in this paper is characterized by a single time scale Δ^{-1} it is natural to assume that the universal dynamics should not depend on these parameters as long as $T_0 \ll \Delta$ and $\tau \ll 1/\Delta$. For the mean-field model (3) this claim can be verified by exact diagonalization, as shown in Fig. 6, or by the semiclassical method introduced above.

For the one dimensional case, one can move one step further and show that a finite T_0 and τ can be used as additional

scaling parameters:

$$C_{12}(t) = \langle \cos(\sqrt{2}\phi(t)) \rangle = \left(\frac{\Delta}{\mu}\right)^{\eta} R\left(\Delta t, \frac{T_0}{\Delta}, \Delta \tau\right) \quad (\text{C1})$$

In particular, this scaling relation confirms that, as long as $T_0 \ll \Delta$ and $\tau \ll 1/\Delta$, the resulting dynamics should be independent on these parameters. To demonstrate the validity of Eq. (C1) and starting from the series expansion presented above, one obtains:

$$C_{12}(t) = \sum_N \frac{(ij_{\perp}\rho_0)^N}{2^N N!} \int_N \epsilon_i \hat{\epsilon}_i f\left(\frac{t_i}{\tau}\right) \langle \exp\left(2i \sum_{i=0}^N \epsilon_i \phi_i + \hat{\epsilon}_i \hat{\phi}_i\right) \rangle_{T_0} \quad (\text{C2})$$

Here f determines the shape of the ramp and satisfies $f(0) = 0$ and $f(x > 1) = 1$, and the expectation value $\langle \dots \rangle_{T_0}$ refers to an equilibrium system at temperature T_0 . If we now rescale the time and space coordinates in units of Δ^{-1} we obtain:

$$\sum_N \frac{(ij_{\perp}\rho_0)^N \Delta^{2N}}{2^N N!} \int_N \epsilon_i \hat{\epsilon}_i f\left(\frac{t_i}{\Delta \tau}\right) \langle \exp\left(2i \sum_{i=0}^N \epsilon_i \phi'_i + \hat{\epsilon}_i \hat{\phi}'_i\right) \rangle_{T_0}, \quad (\text{C3})$$

where we define $\phi'_i = \phi(\Delta x_i, \Delta t_i)$. Due to the scale invariance of the underlying theory (and provided that $T_0 \ll \mu$) we have that

$$\langle \phi'_i \phi'_j \rangle_{T_0} \approx \langle \phi_i \phi_j \rangle_{T_0/\Delta} + \frac{1}{8K} \log\left(\frac{\Delta}{\mu}\right) \quad (\text{C4})$$

Combining this result with Eq. (C3) one can easily show the validity of the generalized scaling relation (C1). This scaling relation is expected to be valid in the mean-field model as well, corresponding to the $K \rightarrow \infty$ limit of the one-dimensional case.

Appendix D: Experimental realization

A natural realization of the proposed experiment involves wave-interferometers of atoms on a chip [40]. This set-up has been successfully used to realize “dephasing” experiments, in which one condensate is suddenly split in two parts [40, 41]. There, the time evolution is described by a gapless Hamiltonian and the resulting dynamics can be studied by the exact solution of the quadratic Luttinger liquid Hamiltonian [27, 41, 47]. Due to the absence of an excitation gap, at long-times the “dephasing” process is primarily thermal, rather than quantum [41, 48]. In contrast, in the present “rephasing” experiment we predict a universal dynamics dominated by quantum effects both at short and long times.

This type of interferometry poses a serious challenge for the observation of one dimensional physics, due to the extremely high value of the Luttinger parameter $K \approx 50$. For this system $\eta = 1/(2K) \approx 0$ and the deviations of the average interference $C_{12}(t)$ from predictions of the two-mode model (2) are extremely small and hard to observe. As suggested in Ref. [27],

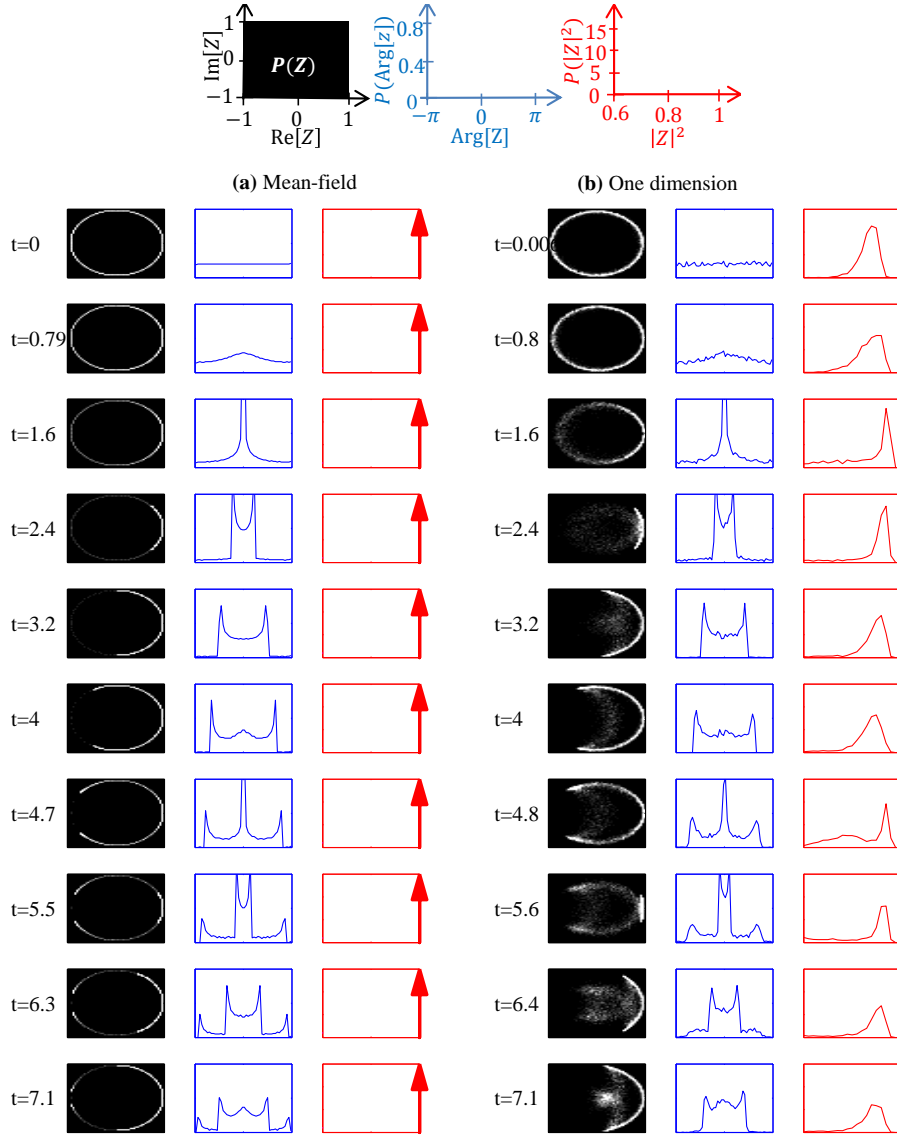


FIG. 7: [Color online] Full distribution function of the spatially integrated coherence (D1), according to the semiclassical equations of motion of (a) the two-mode model and (b) the one dimensional model (11). Both subplots represent in the first column a colorplot of the distribution function of Z on the imaginary plane. In the second column, the distribution function of the phase of Z . In the third column, the distribution function of the absolute value square of Z . Numerical values – (a) $j_{\perp}/\mu = 0.1$, time is given in units of the inverse plasma frequency $\Delta = 2(j_{\perp}\mu)^{-1/2}$. (b) $j_{\perp}/\mu = 0.1$, $K = 25$, $L = 400$, corresponding to the scaling limit $j_{\perp}/\mu \ll 1$, $K \gg 1$, $\Delta L \gg 1$. Time is given in units of the inverse gap $\Delta^{-1} \approx ((4\pi/K)j_{\perp}\rho_0)^{-1/2}$.

the one dimensional nature of the problem can be observed by probing the spatially integrated coherence

$$Z = \frac{1}{L} \int_{-L/2}^{L/2} dx e^{i\sqrt{2}\phi(x,t)}, \quad (\text{D1})$$

where L is the system size. In the two subplots of Fig. 7 we compare the evolution of the full-distribution function of Z for respectively the two-mode and the one-dimensional models. In each subplot, the first column contains a colorplot, proportional to the probability of observing a specific complex value of the operator Z . The second column refers to the

phase of Z . The two-mode and one-dimensional cases look identical for short times, but differ at longer times. In particular, the side-peaks at $\phi \approx \pm\pi$ disappear as a consequence of the one dimensional dynamics. The third column represents the probability distribution of the absolute value of Z . For the two-mode case, it simply corresponds to a delta-function peak at the maximal value of $|Z| = 1$. In contrast, for the one-dimension case $P(|Z|)$ oscillates between the initial Gumbel distribution and narrower peaks, indicating the formation of long-range order in the relative phase.

-
- [1] A. Mitra, S. Takei, Y. B. Kim, and A. J. Millis, *Phys. Rev. Lett.* **97**, 236808 (2006).
- [2] S. Diehl, A. Micheli, A. Kantian, B. Kraus, H. P. Buchler, and P. Zoller, *Nature Physics* **4**, 878 (2008).
- [3] E. G. Dalla Torre, E. Demler, T. Giamarchi, and E. Altman, *Nature Physics* **6**, 806 (2010).
- [4] A. Polkovnikov, K. Sengupta, A. Silva, and M. Vengalattore, *Rev. Mod. Phys.* **83**, 863 (2011).
- [5] L. V. S. Deng, G. Ortiz, *Europhys. Lett.* **84**, 67008 (2008).
- [6] C. De Grandi, A. Polkovnikov, and A. W. Sandvik, *Phys. Rev. B* **84**, 224303 (2011).
- [7] A. Chandran, A. Erez, S. S. Gubser, and S. L. Sondhi, *Phys. Rev. B* **86**, 064304 (2012).
- [8] M. Kolodrubetz, B. K. Clark, and D. A. Huse, *Phys. Rev. Lett.* **109**, 015701 (2012).
- [9] C. De Grandi, V. Gritsev, and A. Polkovnikov, *Phys. Rev. B* **81**, 012303 (2010).
- [10] L. Campos Venuti and P. Zanardi, *Phys. Rev. A* **81**, 032113 (2010).
- [11] D. Iyer and N. Andrei, *Phys. Rev. Lett.* **109**, 115304 (2012).
- [12] C. Karrasch, J. Rentrop, D. Schuricht, and V. Meden, *Phys. Rev. Lett.* **109**, 126406 (2012).
- [13] C. Neuenhahn, A. Polkovnikov, and F. Marquardt, *Phys. Rev. Lett.* **109**, 085304 (2012).
- [14] H. K. Janssen, B. Schaub, and B. Schmittmann, *Zeitschrift fur Physik B Condensed Matter* **73**, 539 (1989), 10.1007/BF01319383.
- [15] B. Zheng, *International Journal of Modern Physics B* **12**, 1419 (1998).
- [16] A. B. Kolton, A. Rosso, E. V. Albano, and T. Giamarchi, *Phys. Rev. B* **74**, 140201 (2006).
- [17] E. V. Albano, M. A. Bab, G. Baglietto, R. A. Borzi, T. S. Grigera, E. S. Loscar, D. E. Rodriguez, M. L. R. Puzzo, and G. P. Saracco, *Reports on Progress in Physics* **74**, 026501 (2011).
- [18] M. J. Steel, M. K. Olsen, L. I. Plimak, P. D. Drummond, S. M. Tan, M. J. Collett, D. F. Walls, and R. Graham, *Phys. Rev. A* **58**, 4824 (1998).
- [19] A. Sinatra, C. Lobo, and Y. Castin, *Phys. Rev. Lett.* **87**, 210404 (2001).
- [20] C. Bodet, J. Estève, M. K. Oberthaler, and T. Gasenzer, *Phys. Rev. A* **81**, 063605 (2010).
- [21] T. Giamarchi, *Quantum Physics in One Dimension* (Oxford University Press, Oxford, 2004).
- [22] F. D. M. Haldane, *Phys. Rev. Lett.* **45**, 1358 (1980).
- [23] P. Calabrese and J. Cardy, *Phys. Rev. Lett.* **96**, 136801 (2006).
- [24] A. Altland and B. Simons, *Condensed Matter Field Theory* (Cambridge University Press, 2010).
- [25] A. Kamenev, *Field Theory of Non-Equilibrium Systems*, 1st ed. (Cambridge University Press, 2011).
- [26] J. Fröhlich and T. Spencer, *Communications in Mathematical Physics* **81**, 527 (1981), 10.1007/BF01208273.
- [27] V. Gritsev, E. Altman, E. Demler, and A. Polkovnikov, *Nature Physics* **2**, 705 (2006).
- [28] L. Mathey and A. Polkovnikov, *Phys. Rev. A* **81**, 033605 (2010).
- [29] A. B. Zamolodchikov, *International Journal of Modern Physics A* **10**, 1125 (1995).
- [30] S. Lukyanov and A. Zamolodchikov, *Nuclear Physics B* **493**, 571 (1997).
- [31] C. De Grandi, V. Gritsev, and A. Polkovnikov, *Phys. Rev. B* **81**, 224301 (2010).
- [32] A. Iucci and M. A. Cazalilla, *New Journal of Physics* **12**, 055019 (2010).
- [33] S. R. White, *Phys. Rev. Lett.* **69**, 2863 (1992).
- [34] U. Schöllwock, *Annals of Physics* **326**, 96 (2011), january 2011 Special Issue.
- [35] H. Bethe, *Zeitschrift fur Physik A Hadrons and Nuclei* **71**, 205 (1931), 10.1007/BF01341708.
- [36] J. Sirker and M. Bortz, *Journal of Statistical Mechanics: Theory and Experiment* **2006**, P01007 (2006).
- [37] G. Vidal, *Phys. Rev. Lett.* **93**, 040502 (2004).
- [38] M. L. Wall and L. D. Carr, *Open Source TEBD (2009)* (<http://physics.mines.edu/downloads/software/tebd/>).
- [39] D. Witthaut, E. M. Graefe, and H. J. Korsch, *Phys. Rev. A* **73**, 063609 (2006).
- [40] T. Schumm, S. Hofferberth, L. M. Andersson, S. Wildermuth, S. Groth, I. Bar-Joseph, J. Schmiedmayer, and P. Kruger, *Nature Physics* **1**, 57 (2005).
- [41] M. Gring, M. Kuhnert, T. Langen, T. Kitagawa, B. Rauer, M. Schreitl, I. Mazets, D. A. Smith, E. Demler, and J. Schmiedmayer, *Science* **337**, 1318 (2012).
- [42] A. Mitra and T. Giamarchi, *Phys. Rev. Lett.* **107**, 150602 (2011).
- [43] E. G. Dalla Torre, E. Demler, T. Giamarchi, and E. Altman, *Phys. Rev. B* **85**, 184302 (2012).
- [44] A. Mitra and T. Giamarchi, *Phys. Rev. B* **85**, 075117 (2012).
- [45] A. Mitra, *Phys. Rev. Lett.* **109**, 260601 (2012).
- [46] A. Luther and I. Peschel, *Phys. Rev. B* **9**, 2911 (1974).
- [47] R. Bistritzer and E. Altman, *Proceedings of the National Academy of Sciences* **104**, 9955 (2007).
- [48] P. Barmettler, M. Punk, V. Gritsev, E. Demler, and E. Altman, *New Journal of Physics* **12**, 055017 (2010).
- [49] A homogeneous tunneling coupling in three dimensions can be realized using two different hyperfine states and suddenly turning-on a frequency-matched microwave coupling.
- [50] The dynamics in the gapped phase has been studied in Ref. [32] by a quadratic expansion of the cosine term. This approach neglects the mode-coupling effect of the cosine and does not capture the rephasing dynamics.
- [51] In actual experiments with soft-core bosons such term is not necessary